Observation of 1/1 impurity-related ideal internal kink mode locking in the EAST tokamak

2013 Plasma Phys. Control. Fusion 55 032001

(http://iopscience.iop.org/0741-3335/55/3/032001)

IOP PUBLISHING PLASMA PHYSICS AND CONTROLLED FUSION

Plasma Phys. Control. Fusion **55** (2013) 032001 (7pp) doi:10.1088/0741-3335/55/3/032001

BRIEF COMMUNICATION

Observation of 1/1 impurity-related ideal internal kink mode locking in the EAST tokamak

Liqing Xu, Liqun Hu, Kaiyun Chen, Erzhong Li, Fudi Wang, Guoqiang Zhong, Yinjie Chen, Ying Xi and the EAST Team

Institute of Plasma Physics, Chinese Academy of Science, PO Box 1126, Hefei 230031, People's Republic of China

E-mail: lqhu@ipp.ac.cn (L Hu)

Received 1 October 2012, in final form 26 December 2012
Published 8 February 2013
Online at stacks.iop.org/PPCF/55/032001

Abstract

$m/n = 1/1$ pressure gradient driven impurity-related ideal internal kink mode locking is observed in EAST limit-cycle state H-mode plasmas. This 1/1 mode has a radial structure with no inversion around the resonance, which implies that the mode has an ideal internal kink structure. The rotation direction of the 1/1 internal kink mode, as obtained by tomography of a high-resolution multi-array soft x-ray system, is the ion diamagnetic drift velocity direction. Impurities accumulated in the central region play a vital role in mode excitation. Remarkable loss of the yield of neutron rate due to 1/1 mode is also observed. A notch at the location in the vicinity of $q = 1$ is also observed in the local toroidal rotation profile. Furthermore, the frequency chirping behavior of the 1/1 kink mode is related to the toroidal rotation velocity of the plasma.

(Some figures may appear in colour only in the online journal)

1. Introduction

In the central region of a tokamak plasma, a kind of magnetohydrodynamics (MHD) instability exhibiting periodic oscillations in experimental manifestation, termed as precursors of sawtooth oscillations [1], fishbone [2], snakes [3, 4] and long-lived modes [5–8], is dominantly associated with helical perturbations having poloidal mode number $m = 1$ and toroidal mode number $n = 1$. The sawtooth oscillations and fishbone were theoretically known to be characteristic of the internal kink mode, a MHD instability that occurs in the vicinity of the $q = 1$ surface. Snakes are large and localized pressure perturbations, which originate from the formation of a small region on the $q = 1$ surface with highly increased density. Snakes are routinely triggered by pellet injection in JET and Tore Supra [3, 4]. In the MAST tokamak, long-lived and saturated ideal MHD instabilities were regularly observed at a safety factor above unity and a profile with either weakly reversed shear or broad low-shear region plasmas [5–7]. After pellet injection, a rich variety of $m = 1$ island dynamics were visible in FTU. Strong rotation braking of the $m = 1$ island was also found in the FTU tokamak [8].

As mentioned above, there are various interesting behaviors of the 1/1 internal mode in tokamaks. One more vital problem is about the frequency chirping of the 1/1 internal mode. It is widely accepted that the frequency chirping of fishbone is associated with energy losses and redistribution of fast particles [9]. However, a recent research result shows that the frequency chirping during fishbone activity can be attributed to the reactive torque exerted on the plasma during the instability burst, which slows down plasma rotation inside the $q = 1$ surface and reduces the mode frequency in the lab frame [10].

Recently, it has been reported that the rotation of the $m/n = 1/1$ ideal interchange mode slowed down and stopped in the Large Helical Device (LHD) [11]. The minor collapse was caused by the growth of the mode just after mode locking.

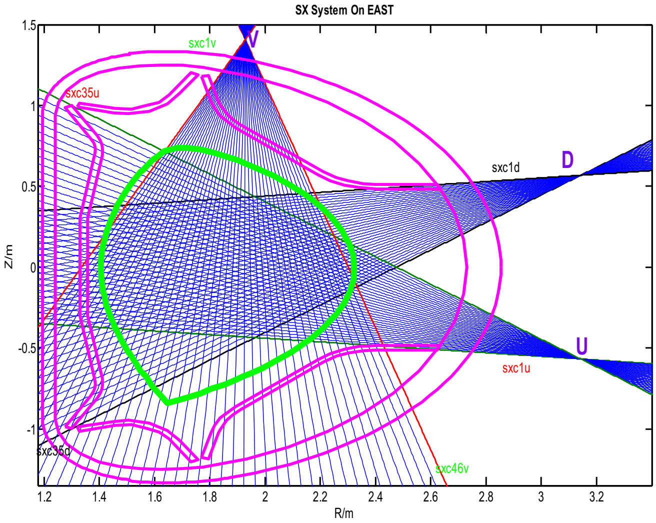

Figure 1. Schematic diagram of the SXR imaging system on the EAST tokamak. Each of U and D arrays has 35 chords that are numbered clockwise from 1 to 35. The V array has 46 chords named from SXC1V to SXC46V.

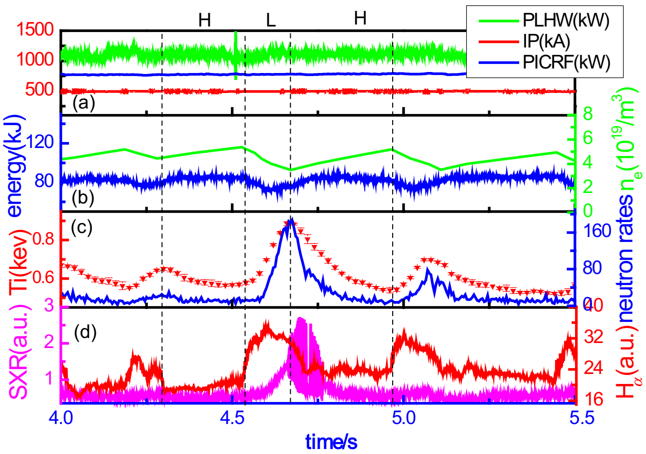

Figure 2. EAST shot #38190 with 1/1 mode locking. In (*a*) the time traces show the auxiliary power (ICRH power in blue and LHW power in purple) and the plasma current (in red). The time slices in (*b*) are the plasma energy (in blue) and the central line-averaged electron density (in green). (*c*) is the time evolution of the central ion temperature T_i (in red) and the yield of neutron (in blue) .Shown in (*d*) are the central SXR radiation (in purple) and the upper divertor H_α emission (in red).

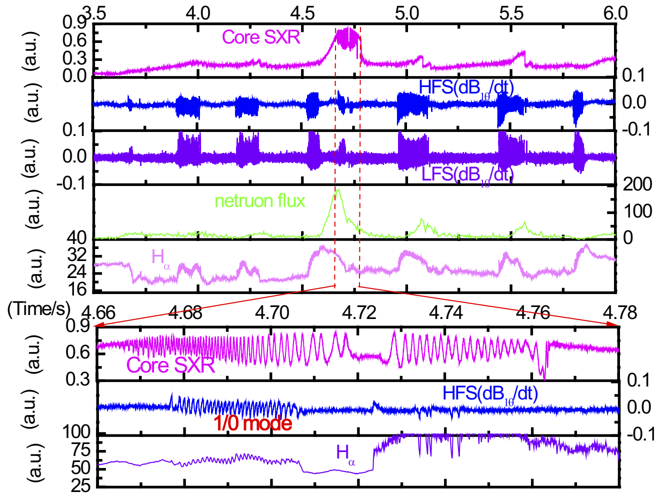

Figure 3. Time traces of shot #38190. Core SXR radiation, magnetic fluctuation in higher field side and lower field side, neutron rates, upper divertor H_α emission. The bottom three slices are the expanding signals. The magnetic oscillations with 1/0 structure are limit-cycle states.

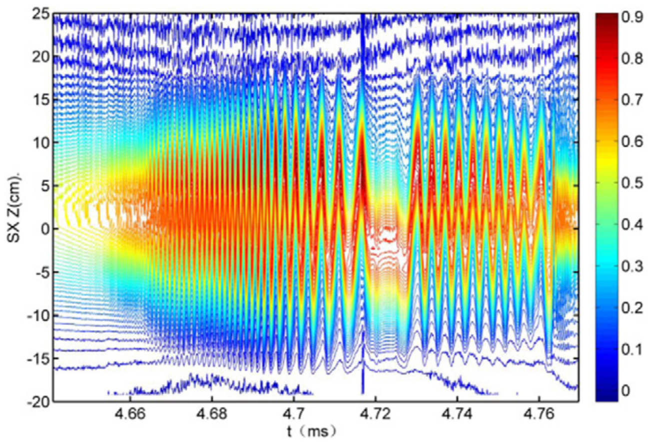

Figure 4. Time–space plot of the 1/1 locked mode. SXR U array shown in figure 1 is employed for the plot.

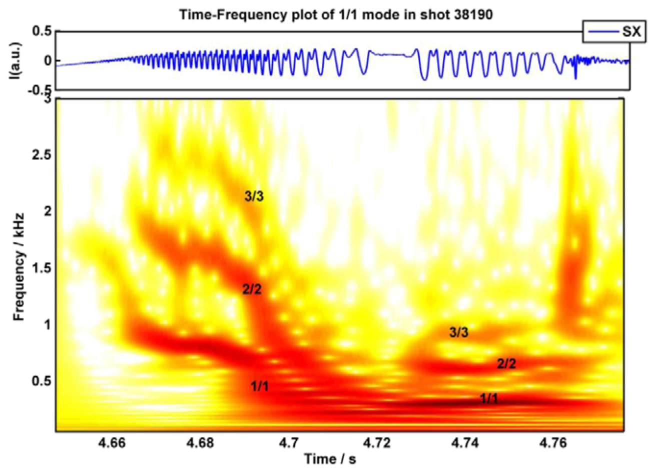

Figure 5. Continuous wavelet transform scalogram of the 1/1 kink mode; top is the SXC10U signal with $r = 0.082$ cm. The frequency of 1/1 drops down to zero.

There was no inversion in the radial structure around the resonance before locking.

In this paper, 1/1 pressure gradient driven internal kink mode locking is observed for the first time in EAST plasmas. Impurity-related ideal 1/1 internal kink mode locking does not lead to hard disruption. Unlike typical of tearing modes, there is no phase inversion in closely placed channels in horizontal soft x-ray (SXR) arrays in this internal kink-mode radial structure. These modes are notable for lack of islands or signs of reconnection, which are consistent with the observations of MAST [7] and LHD [11]. It is also found that the frequency chirping behavior of 1/1 modes is related to the toroidal rotation of the plasma.

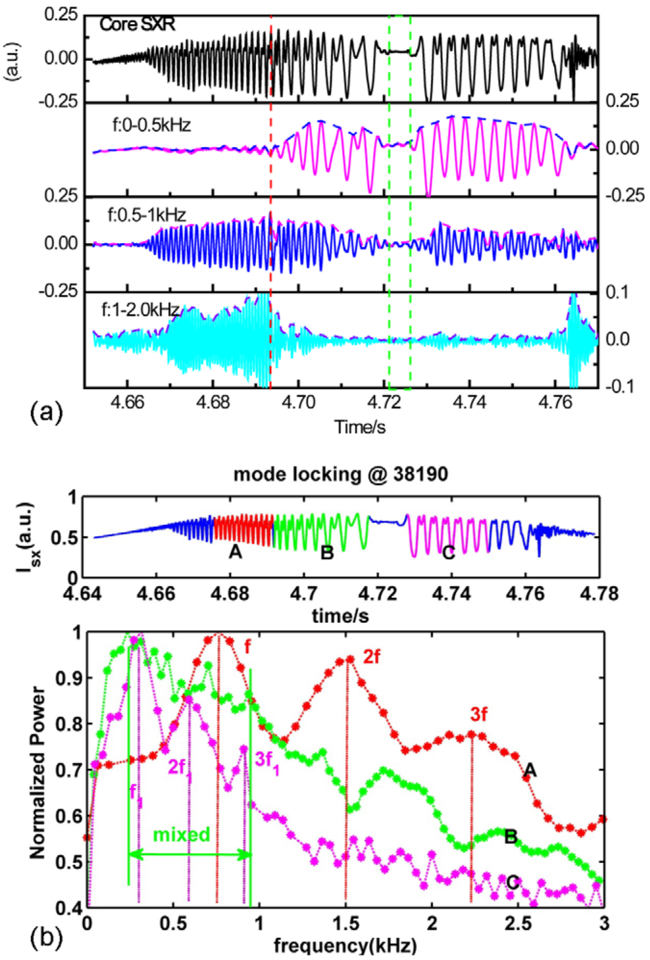

Figure 6. Time evolution of 1/1 internal kink mode. (*a*) Raw and filtered SXR signals showing the evolution of amplitudes with different frequency ranges. The horizontal dashed lines correspond to the amplitudes of specific signals. The red dashed vertical line indicates that strong frequency chirping started at time point $t = 4.693$ s before mode locking. (*b*) Top is the central SXR signal and the bottom one is the normalized spectral amplitude. The spectrum becomes broad in the B phase. The harmonic modes are shown clearly both in phases A and C; $f \approx 0.75$ kHz, $2f \approx 1.5$ kHz and $3f \approx 2.25$ kHz before mode locking; $f_1 \approx 0.3$ kHz, $2f_1 \approx 0.6$ kHz and $3f_1 \approx 0.9$ kHz just after mode locking.

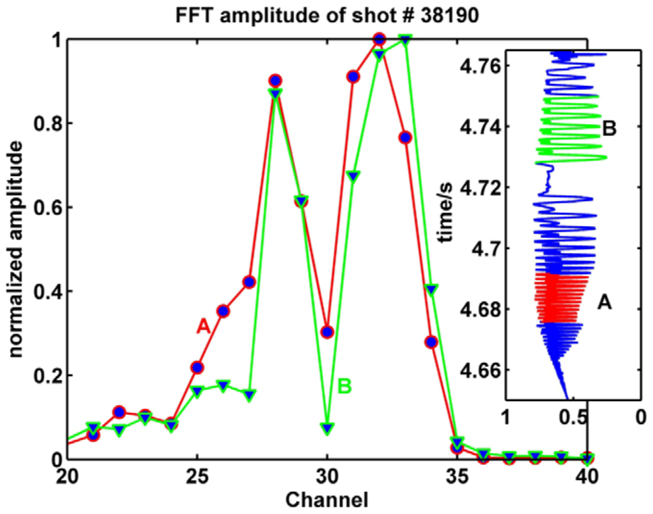

Figure 7. Determination of poloidal mode numbers before and after mode locking by the FFT method. FFT amplitude of the line-integrated SXR signals is plotted versus the SXR line channels for 1/1 modes. The dominant modes before locking and after locking are the $m = 1$ modes.

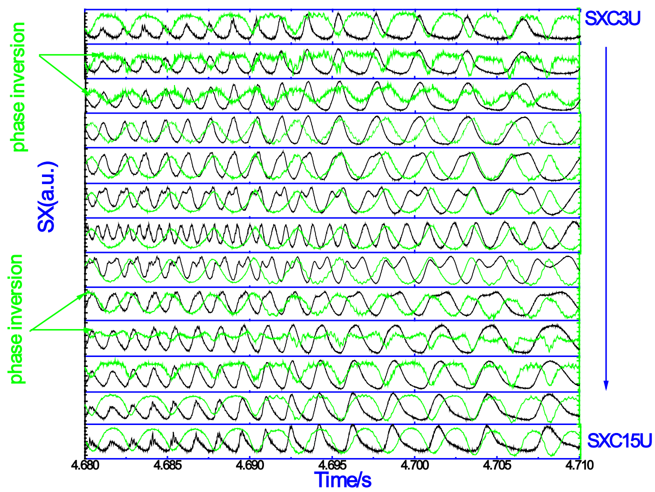

Figure 8. Comparison of horizontal SXR array signals between a typical tearing mode and the 1/1 kink mode. In green is the tearing mode with phase inversion. In black is the 1/1 kink mode.

The rest of this paper is organized as follows. The following section describes the diagnostics and experiments. In section 3, an overview of the experimental observations is presented. A discussion on the driving force and frequency chirping behavior of the 1/1 internal kink mode is presented in section 4. Finally, the main points are summarized in section 5.

2. Experimental set-up

The results presented in this paper were obtained in the latest lower hybrid current drive (LHCD) and ion cyclotron range of frequency (ICRF) cooperative experiments on EAST, the world's first noncircular cross-section full superconducting tokamak (major radius $R = 1.70$ m, typical minor radius $a = 0.40$ m) [12]. In the 2012 experimental campaigns, the lower hybrid waves (LHWs) were injected by a 20 waveguide launcher capable of delivering up to 2 MW of power at 2.45 GHz with a $n_{\parallel}$ value 2.1 directed to the drive current parallel to I_p, the toroidal plasma current [12]. Here $n_{\parallel}$ is the refractive index of the injected LHWs parallel to the magnetic field. The ICRF heating system is not only the heating method but also the current drive for EAST, with two dedicated horizontal ports, named I and O. The range of ICRF is from 25 to 70 MHz, covering all relevant heating scenarios for the toroidal magnetic field $1.5\,\mathrm{T} < B_0 < 3.5$ T: minority heating of H (above 1.6 T) and He^3 (above2.5 T) as well as second harmonic heating of H (below 2.5 T) and He^3 (below 3.5 T). There are four ICRF transmitters [13] on EAST. All four 1.5 MW ICRF transmitters with a frequency range 25–70 MHz were put into operation in the 2012 experimental campaigns.

The toroidal rotation velocity in the core region presented is based on the Doppler shifts and broadening of line emission

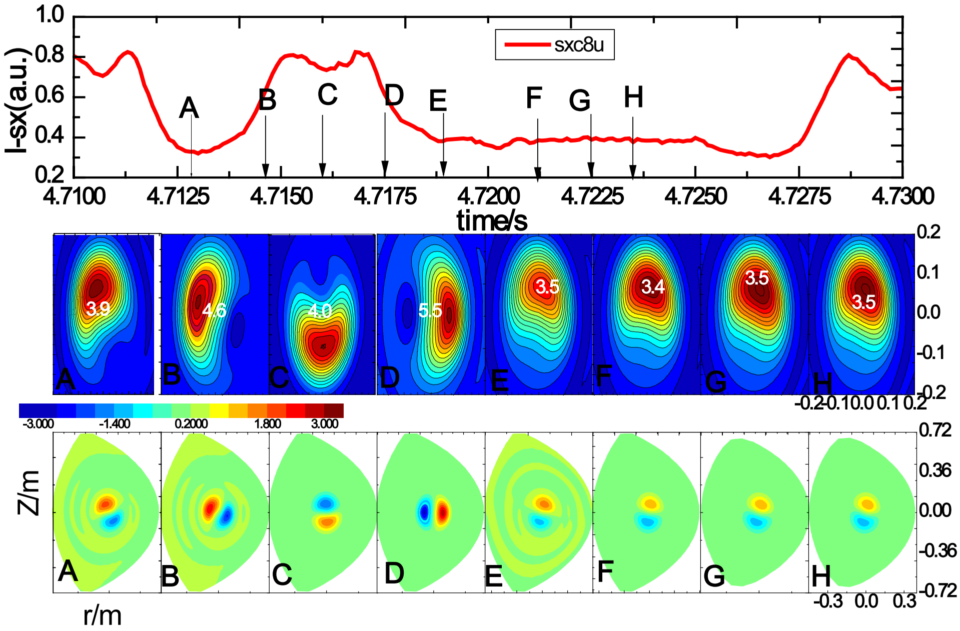

Figure 9. Reconstructed 1/1 mode periodic pictures using tomography of SXR signals. The top row shows the evolution of the line-integrated SXR signals at the central chord. The middle row is the contour plot of the reconstructed local emission intensity profile from the total signals, and the bottom row is the contour plot of the reconstructed perturbation of the local emission intensities from the perturbation signals extracted by the SVD method. The capital letters on the left of the reconstructed frames correspond to those in the top row frames.

from trace amounts of highly ionized argon, measured by a high-resolution imaging x-ray crystal spectrometer (XCS) [14]. The electron temperature is presented by means of a SXR pulse height analysis (PHA) system, based on a silicon drift detector (SDD) measuring the spectra of SXR emission [15]. The 1/1 kink mode is shown and analyzed mainly with SXR signals. The arrangement of the three SXR cameras is shown in figure 1. The cameras are installed in port C of the tokamak. The beryllium window thickness is 12.5 μm. The spatial resolution is 2.5 cm in the central region. The maximum sampling rate is 100 kHz [16].

The poloidal number m of the limit-cycle state is measured using a set of 37 Mirnov probes, localized in the poloidal cross-section, and the toroidal number n of the limit-cycle state is determined using another set of 16 Mirnov probes (MITAB–MITPA), localized in the vessel. The sampling frequency limit for all magnetic measurements is 100 kHz.

3. Experimental observations

A typical H-mode [17] discharge numbered 38190 with 1/1 kink mode instabilities is shown in figure 2. The plasma current I_p is about 500 kA. The auxiliary power values of LHW and ICRF are 1 MW and 0.7 MW, respectively. The edge safety factor is $q_a = 4.5$. The electron density increased rapidly in the H-mode plasma. Due to the increased density, the radiation of plasma enhanced and the plasma energy decreased, hence an H–L transition. In this paper, we do not focus on the intermittent H-mode phase and edge-localized modes (ELMs) as well as H–L transitions. We will pay attention to the 1/1 mode, which follows the L–H transition. This mode has very localized pressure perturbation. Furthermore, both the yield of neutron rates and the SXR radiation increase originate from impurity accumulation and the increased ion density before the onset of the 1/1 kink mode. After 1/1 mode destabilization, the neutron rates decreased, which implies the enhanced loss of neutron rates due to 1/1 instability. In addition, the 1/1 mode located inside $q = 1$ in the plasma, however 1/0 oscillations are regularly detected on the edge, where the magnetic coils are located, as shown in figure 3. These 1/0 oscillations are not the edge magnetic structure associated with the 1/1 kink mode. The 1/0 oscillation, termed the limit-cycle state, following the L–H transition with small amplitude and low-frequency oscillation is related to the interactions between zonal flows and high-frequency turbulences at the pedestal [18].

From figure 4, the time–space plots of SXR signals, it is clear that the frequency of the kink mode drops to 0 and the stopping of the rotation of the 1/1 hot core lasts for about 5 ms. Furthermore, after locking, the rotation of the hot core recovers to a quasi-steady frequency. Tomography of SXR will give more details about the rotation behavior of the hot core. The continuous wavelet transform method is used for the time–frequency plot in figure 5. Based on the optimized and localized function of the wavelet, the scalogram provides the instantaneous frequency spectrum of the random signal as well as the time-dependent amplitudes of each frequency component. From figure 5, the frequencies of the 1/1 and higher harmonic modes chirp down before mode locking. However, the frequencies of the 1/1, 2/2 and 3/3 modes are constant after mode locking.

The dynamic characteristic of the different frequency signals could be extracted by the fast Fourier transform (FFT) filtering method. The results are illustrated in figure 6(a). Because of the strong frequency chirping of the 1/1 mode,

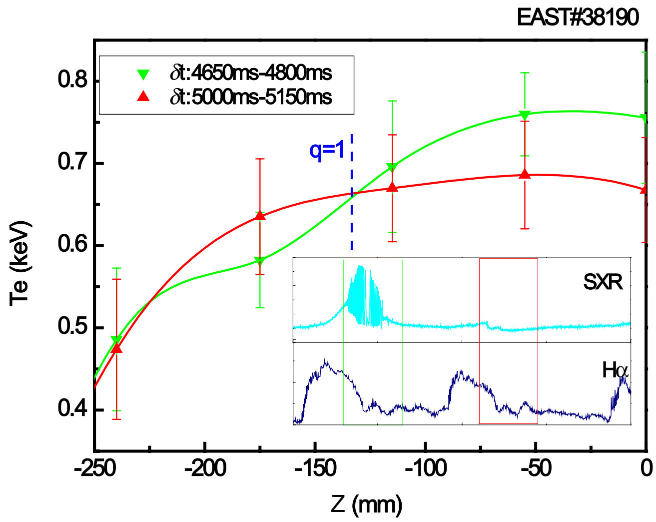

Figure 10. Profiles of electron temperature of EAST shot #38190. The profile was peaked in an ELM-free H-mode plasma with 1/1 kink mode. Green profile with 1/1 and red profile without, as shown in the inner axes. The temperature is measured by the SXR PHA system. The blue dashed line indicates the $q = 1$ surface.

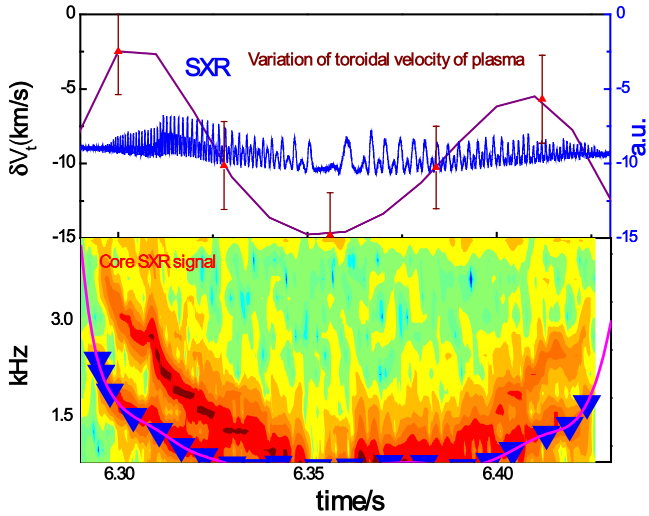

Figure 12. Time evolution of the relative toroidal rotation velocity of an EAST plasma shot #38512. U-font-style sweeping of 1/1 mode frequency and relative toroidal rotation velocity. The rotation velocity is relative to the time point $t = 5.0$ s. The rotation velocity taken at a particular radial location $Z = 9$ cm.

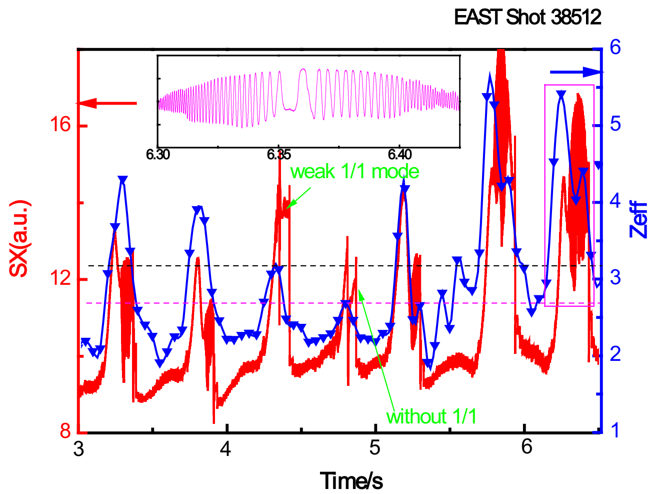

Figure 11. Another typical EAST shot #38512 with 1/1 mode locking. The red signal is SXR radiation and the blue is the effective charge Z_{eff}. It is apparent that there is a critical value Z_{eff} to excite the 1/1 kink mode. Shown in the inner frame is the expanding SXR signal, which is the signal in the dominant frame highlighted with a purple rectangle.

it is difficult to discern the dynamic characteristic of the 1/1 and higher harmonic modes just before mode locking. However, FFT can also be used to clearly see the dynamic characteristics of different frequency signals. The signal with a frequency range from 0 to 0.5 kHz begins at time point $t = 4.693$ s when the strong frequency chirping before the onset of mode locking. Moreover, the mode locking lasts for about 5 ms, which is shown in figure 6(*a*) highlighted with a green rectangle. Signals with different frequency ranges co-exist both before and after mode locking. Due to the limitations of the FFT method in frequency resolution, a compounded spectrum is observed in phase B for 1/1 and 2/2 modes with strong frequency chirping and there is only a small discrepancy in frequency between them, as shown in figure 6(*b*). In addition, three coherent peaks with mode numbers 1/1, 2/2 and 3/3, respectively, are marked in the normalized power spectra both in phases A and C. The spatial structure of the kink mode is analyzed by means of the FFT method. The results in figure 7 indicate that the dominant modes are $m = 1$ both before and just after locking.

Figure 8 indicates that the 1/1 mode before mode locking seemingly has an ideal internal kink-mode structure (not a magnetic island), as can be deduced from the horizontal array showing no phase inversion in closely placed channels. A typical tearing mode with phase inversion in closely placed channels of the SXR array is also presented in figure 8 in green for comparison.

Using tomography, the emission profile evolution reconstructed from the perturbation signals of the ideal 1/1 kink mode is shown in the bottom frames in figure 9. Apparently, the poloidal mode number of this kink mode is $m = 1$. From the middle row (figure 9(C)), a large displacement due to the shift of the 1/1 kink mode is visible. The rotation direction of the 1/1 kink mode is the counterclockwise direction, which is consistent with the direction of the ion diamagnetic drift. The rotation frequency is the oscillation frequency of SXR signals. In addition, the 1/1 mode locking lasts for only about 5 ms; after mode locking, the rotation of the 1/1 mode recovers. The rotation direction of the 1/1 mode after mode locking is also in the direction of ion diamagnetic drift.

4. Discussion on the driving force and frequency chirping behavior of the 1/1 internal kink mode

By means of the SXR PHA diagnostic, close examination of medium-Z impurities as well as measurements of T_e values were conducted on EAST. From figure 10, it is clear that the temperature profile is flat in the core region in the ELM-free H-mode plasma. However, due to the accumulation of

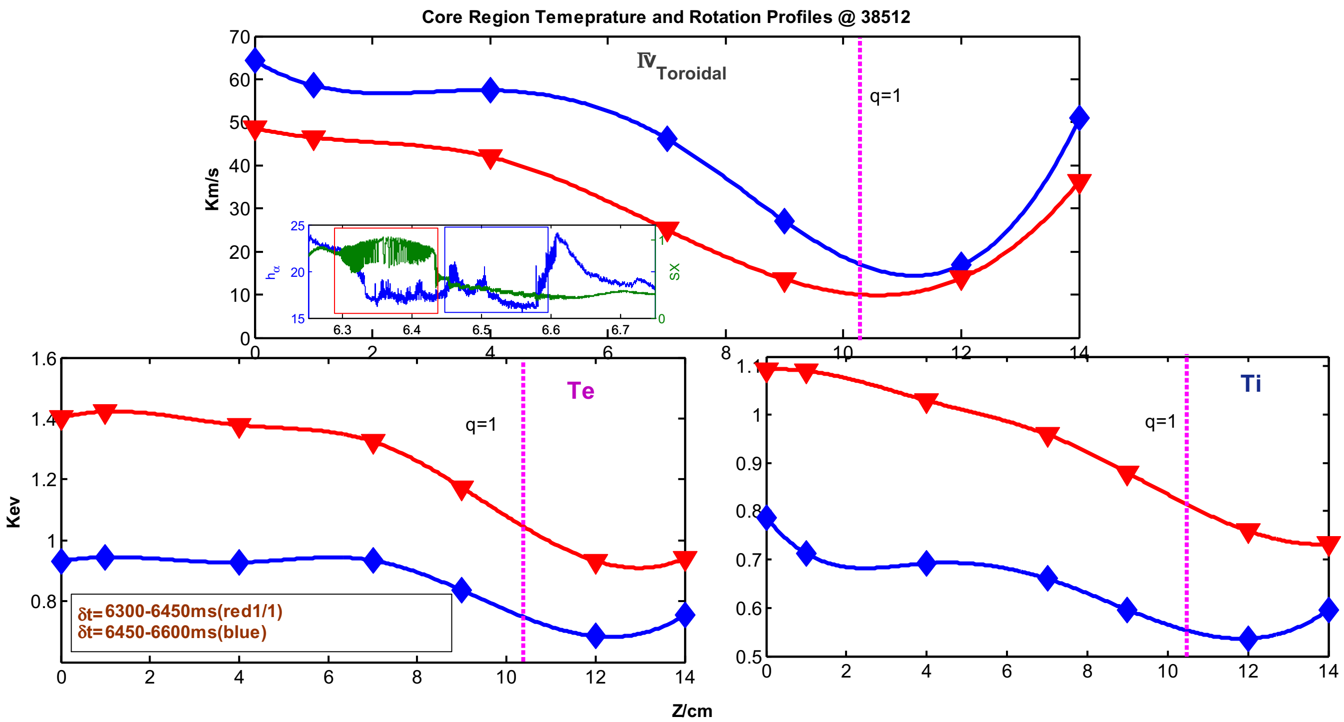

Figure 13. Profiles of electron and ion temperatures and toroidal rotation. The temperature of electrons and ions increased and the toroidal rotation decreased during the 1/1 mode burst. The profiles of electrons and ions become peaked in the $q = 1$ region. A notch at the location in the vicinity of $q = 1$ is visible in the local toroidal rotation profile. The rotation velocity is relative to the time point $t = 7.5$ s when the discharge is almost at the end; the rotation of the plasma can be treated roughly as zero. The toroidal rotation velocity of the plasma, electron temperature and ion temperature were measured by a high-resolution imaging x-ray crystal spectrometer.

impurities and increased electron density, the SXR radiation is enhanced, and the electron temperature is decreased in the core region. These observations imply the existence of local improvement of confinement. And above all, the temperature profile becomes more steep in the vicinity of $q = 1$ where the 1/1 internal kink takes place. There is no 1/1 mode burst due to the flattened temperature profile in the vicinity of $q = 1$, as shown in figure 10, which is highlighted with a red rectangle.

In EAST shot #38512, U-font-type sweeping of the 1/1 internal kink mode frequency behavior is consistent with the relative toroidal rotation velocity of the plasma, as shown in figure 12. The toroidal rotation velocity is relative to the rotation velocity at time point $t = 5.0$ s. Furthermore, it is observed that the temperature of both electrons and ions increased and the toroidal rotation velocity of the plasma decreased in the plasma central region. The same phenomenon, i.e. the toroidal rotation decreased (the profile flattened in the core region) in the plasma core region where 1/1 mode burst took place, was also observed in MAST [6]. There are also larger gradients of both electron and ion temperature profiles in the vicinity of $q = 1$ where 1/1 mode occurs, as shown in figure 13. Furthermore, a notch at the location in the vicinity of $q = 1$ is observed in the local toroidal rotation profile, which implies that apparently there is a weak flow shear in the $q = 1$ region. In addition, a notch of toroidal rotation profile was also reported by Shirai *et al* in an LHD internal transport barrier formation plasma [19]. All of these observations demonstrate that the frequency chirping of the 1/1 mode originates from the toroidal rotation and plasma flow.

Another example shot with 1/1 mode locking is shown in figure 11. Obviously, the destabilization of the 1/1 mode is related to the accumulation of impurities in the plasma core region.

5. Summary

It is the first time that impurity-related ideal 1/1 internal kink mode locking was observed in EAST tokamak plasmas. 1/1 internal kink mode locking does not lead to hard disruption. 1/1 mode and its harmonic modes co-exist both just before and just after mode locking. The rotation direction of the 1/1 mode is the ion diamagnetic direction. The pressure gradient is the most probable driving force of the 1/1 internal kink mode (the pressure driven internal kink is also called the quasi-interchange). The large accumulation of impurities is related to the pressure gradient in the $q = 1$ region. The frequency chirping behavior of the 1/1 mode is related to the toroidal rotation velocity of the plasma and plasma flow.

Acknowledgments

This work was partially supported by the JSPS-NRF-NSFC A3 Foresight Program in the field of Plasma Physics (NSFC No 11261140328). This work was partially supported by the National Nature Science Foundation of China through grant numbers 10935004, 11205007, 10975155, 10990212, and was partially supported by the CAS Key International S&T Cooperation Project collaboration with grant number

GJHZ1123. The authors gratefully acknowledge the fruitful discussions with D V Igochine (MPI fur Plasmaphysik, Euratom-Association, Germany).

References

[1] vonGoeler S, Stodiek W and Sauthoff N 1974 *Phys. Rev. Lett.* **33** 1201
[2] McGuire K *et al* 1983 *Phys. Rev. Lett.* **50** 891
[3] Gill R D *et al* 1992 *Nucl. Fusion* **32** 723
[4] Pecquet A L *et al* 1997 *Nucl. Fusion* **37** 451
[5] Gryaznevich M P 2008 *Nucl. Fusion* **48** 084003
[6] Chapman I T *et al* 2010 *Nucl. Fusion* **50** 045007
[7] Chapman I T *et al* 2011 *Nucl. Fusion* **51** 073040
[8] Giovannozzi E *et al* 2004 *Nucl. Fusion* **44** 226–31
[9] Pinches S D *et al* 2004 *Plasma Phys. Control. Fusion* **46** S47
[10] Marchenko V S and Reznik S N 2011 *Nucl. Fusion* **51** 122001
[11] Takemura Y *et al* 2012 *Nucl. Fusion* **52** 102001
[12] Wan B for the EAST and HT-7 Teams and International Collaborators 2009 *Nucl. Fusion* **49** 104011
[13] Zhang X J *et al* 2012 *Nucl. Fusion* **52** 032002
[14] Shi Y *et al* 2010 *Plasma Phys. Control. Fusion* **52** 085014
[15] Xu P *et al* 2010 *Plasma Phys. Control. Fusion* **52** 075013
[16] Chen K, Hu L, Duan Y, Ma T and the HT-7 Team 2010 *Phys. Lett.* A **374** 1849–54
[17] Xu G S *et al* 2011 *Nucl. Fusion* **51** 072001
[18] Wang H Q 2012 *Nucl. Fusion* **52** 123011
[19] Shirai H *et al* 2000 *Plasma Phys. Control. Fusion* **42** 109